



## Suzaku observation of the eclipsing high mass X-ray binary pulsar XTE J1855-026

JINCY DEVASIA<sup>1,2,\*</sup> and BISWAJIT PAUL<sup>1</sup>

<sup>1</sup>Raman Research Institute, Bangalore 560 080, India.

<sup>2</sup>Henry Baker College, Melukavu, Kottayam 686 652, India.

\*Corresponding author. E-mail: jincydevasia@yahoo.com

MS received 31 August 2017; accepted 17 October 2017; published online 9 February 2018

**Abstract.** We report results from analysis performed on an eclipsing supergiant high mass X-ray binary pulsar XTE J1855-026 observed with the X-ray Imaging Spectrometer (XIS) on-board Suzaku Observatory in April 2015. Suzaku observed this source for a total effective exposure of  $\sim 87$  ks just before an eclipse. Pulsations are clearly observed and the pulse profiles of XTE J1855-026 did not show significant energy dependence during this observation consistent with previous reports. The time averaged energy spectrum of XTE J1855-026 in the 1.0–10.5 keV energy range can be well fitted with a partial covering power law model modified with interstellar absorption along with a black-body component for soft excess and a gaussian for iron fluorescence line emission. The hardness ratio evolution during this observation indicated significant absorption of soft X-rays in some segments of the observation. For better understanding of the reason behind this, we performed time-resolved spectroscopy in the 2.5–10.5 keV energy band which revealed significant variations in the spectral parameters, especially the hydrogen column density and iron line equivalent width with flux. The correlated variations in the spectral parameters indicate towards the presence of clumps in the stellar wind of the companion star accounting for the absorption of low energy X-rays in some time segments.

**Keywords.** X-ray; neutron stars—X-ray binaries: individual (XTE J1855-026).

### 1. Introduction

Supergiant High Mass X-ray Binary systems (SgHMXBs) are a sub-class of High Mass X-ray Binary systems (HMXB) consisting of a massive, late type companion star and a neutron star, orbiting about the common center of mass. In most cases, the basic source of power is by the accretion of material via the stellar wind of the binary companion. In wind-fed system, the dense stellar wind of the massive star is partly intercepted by the strong gravitational field of the compact companion and accretion takes place. The orbital period of these systems is in the range of  $P_{\text{orb}} \sim 1\text{--}42$  days. The massive stars in these systems which are of OB spectral type exhibit strong radiatively-driven stellar winds with mass loss rate of the order of  $\sim 10^{-6} M_{\odot} \text{ yr}^{-1}$  and wind terminal velocities of  $\sim 1500 \text{ km s}^{-1}$ . The observed X-ray luminosity from these sources ranges from  $L_x \sim 10^{35}\text{--}10^{36} \text{ ergs s}^{-1}$ , which modifies the stellar wind significantly.

Generally two kinds of sgHMXBs are observed: classical sgHMXBs and heavily obscured sgHMXBs, in which the latter ones are much more absorbed in X-rays ( $N_{\text{H}} > 10^{23} \text{ cm}^{-2}$ ) on average, ten times larger than in classical systems and well above the galactic systems (Manousakis *et al.* 2014). SgHMXBs are known to be persistent sources on longer timescales, although exhibiting significant variabilities on short timescales (Haberl *et al.* 1989). These variabilities are generally attributed to the inhomogeneities in the stellar wind. Eclipsing SgHMXBs are suitable candidates for determining the orbital parameters of the binary system. Apart from that, it also helps in understanding the nature of the circumstellar material of the companion star, especially by analysing the data during eclipse ingress/egress when much of the emission from the compact object is eclipsed and only the reprocessed emission is detectable.

XTE J1855-026 is an eclipsing SgHMXB discovered with *Rossi X-ray Timing Explorer (RXTE)* satellite

in 1998 while scanning across the Scutum region of the Galactic plane. Follow up observations with *RXTE*-PCA instrument revealed the compact object to be a neutron star with a spin period of  $361.1 \pm 0.4$  s and a periodic intensity modulation of 6.1 days interpreted as the orbital period of the system. The source was then identified as a supergiant wind accretion-driven system. The X-ray spectrum of this source above  $\sim 3$  keV was fitted with an absorbed power-law model with a high energy cut-off and a Gaussian line for accounting iron fluorescent emission line at 6.4 keV (equivalent width  $\sim 360$  eV) (Corbet *et al.* 1999). The pulse timing studies of the source using observations made with *RXTE*-PCA obtained a mass function of  $\sim 16M_{\odot}$  for the companion star and constrained the eccentricity to  $e \leq 0.04$  (Corbet & Mukai 2002). Analysis of the spectra of the optical counterpart taken in August 2003 with the 4.2-m WHT (La Palma) showed it to be a B0Iaep luminous supergiant (Negueruela *et al.* 2008). In 2010, *INTEGRAL*-IBAS detected a bright flare from this source in the 20–40 keV X-ray energy range. They observed three flares separated by a spin period of 360 s. Each flare lasted for 130 s, 55 s and 80 s with a peak luminosity of 0.9 Crab, 0.7 Crab and 0.3 Crab, respectively (Watanabe *et al.* 2010). Then in 2012, the *Swift*-BAT hard X-ray transient monitor reported an outburst from this source during which the X-ray intensity increased from its normal level of  $\sim 10$  mCrab in the 15–50 keV band to a level of  $\sim 50$  mCrab over a period of one day (Krimm *et al.* 2012). Using archival *INTEGRAL* dataset, the eclipse duration was estimated to be  $1.08 \pm 0.03$  days (Falanga *et al.* 2015). Gonzalez-Galan (2015) updated the spectral type of the mass donor to a B0.2 Ia supergiant and found the mass and radius of the donor star to be  $\sim 13M_{\odot}$  and  $\sim 27R_{\odot}$  respectively.

Here, we present further studies on this source by using observations made with XIS instrument on-board *Suzaku* Observatory. The observation was carried out in the last stages of the *Suzaku* mission. XTE J1855-026 was observed in 2015 April when the source was just before an eclipse. The following sections focus on the results obtained by studying the pulse profiles and spectral characteristics of this source.

## 2. Observations and analysis

*Suzaku* (Mitsuda *et al.* 2007) is a joint Japanese–US mission launched in 2005 and covers a broad energy range from 0.2 to 600 keV. The mission is declared complete in 2015 after it was successfully operated for about 10 years. The scientific payload comprises of two

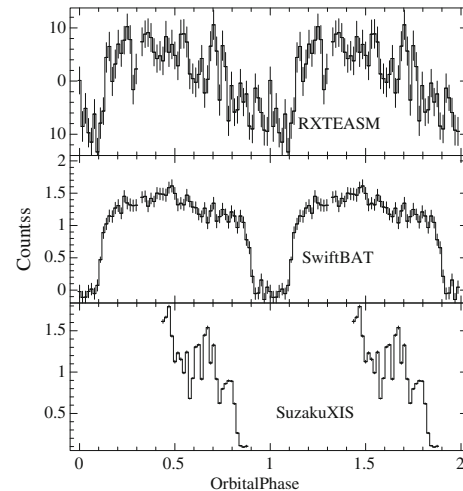


**Figure 1.** The *top panel* shows the *RXTE*-ASM light curve of XTE J1855-026 in the 2–15 keV energy band, the *middle panel* shows the 15–50 keV light curve from the *Swift*-BAT all sky monitor and the *bottom panel* shows the *Suzaku*-XIS light curve in the energy range 0.3–12 keV light curve, all folded with a bin size same as the orbital period of the binary system.

co-aligned instruments: the X-ray Imaging Spectrometer (XIS: Koyama *et al.* 2007) sensitive in the energy band of 0.2–12 keV, and the Hard X-ray Detector (HXD: Takahashi *et al.* 2007) sensitive in the energy band 10–70 keV. The XIS consists of four imaging CCD cameras, each located at the focal plane of an X-ray Telescope (XRT). Three CCD cameras (XIS0, XIS2, XIS3) are front-illuminated and one CCD camera (XIS1) is back-illuminated, out of which three XIS units (XIS0, XIS1 and XIS3) are currently operational. The HXD consists of two instruments – silicon PIN diodes (HXD/PIN) and GSO crystal scintillators (HXD/GSO), working in 10–70 keV and 40–600 keV ranges respectively. For the analysis discussed in this paper, we have used data obtained with the *Suzaku*-XIS instrument. Unfortunately, the HXD data was not available for this particular observation as the HXD instrument was turned off due to decline in the electric power supply.

*Suzaku* observed XTE J1855-026 from 2015-04-22T17:06:19 (MJD 57134.71271991) to 2015-04-25T08:17:15 (MJD 57137.34531250). The observation was performed in XIS nominal pointing in standard data mode with an effective exposure of  $\sim 87.5$  ks. XIS detectors were operated in the ‘normal’ clockmode with ‘1/4’ window option providing 2 s time resolution. We have used publicly available archived data from HEASARC with ObsId-409022010. The analysis discussed in this paper was performed using HEASOFT software package version 6.19 and CALDB database released on

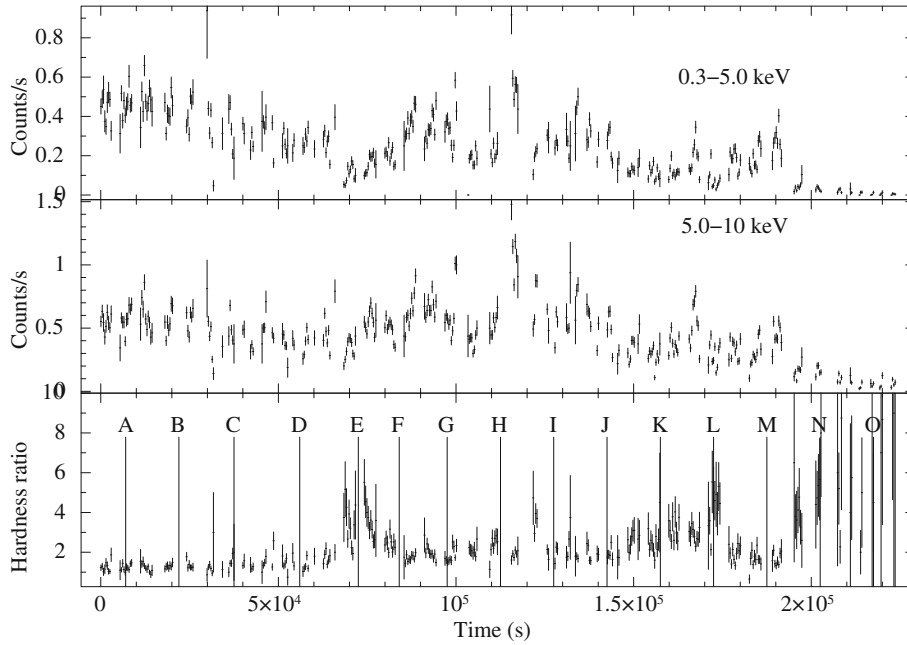


**Figure 2.** The background subtracted light curves of XTE J1855-026 observed with *Suzaku*-XIS. The *top panel* shows the XIS light curve plotted in the 0.3–5 keV energy range, the *middle panel* shows the XIS light curve plotted in the 5–12 keV energy range, and the *bottom panel* shows the hardness ratio plot in these two energy ranges.

2016-06-07. We have used filtered cleaned event files which are obtained using the pre-determined screening criteria as suggested in the *Suzaku* ABC guide<sup>1</sup>. For extracting XIS light curves and spectrum from the cleaned XIS event files, circular regions of 1.2 arcmin (72 arcsec) radius around the source centroid is chosen. The background light curves and spectra were also extracted by using the same selection criteria as for the source by choosing regions devoid of source photons.

Figure 1 shows the orbital intensity light curve of XTE J1855-026 folded with the orbital period of the pulsar, 6.074 days with mid-eclipse epoch chosen to be  $T_{\text{mid}} = \text{MJD } 55079.055$  (Coley *et al.* 2015). The *Suzaku* light curve plotted with the *RXTE*-ASM and *Swift*-BAT long-term light curves indicates that the *Suzaku* observation was carried out when the source is just before an eclipse covering the binary orbital phase range roughly from 0.45–0.85. The long-term light curves show significant energy dependence and we noticed significant reduction in source flux even before the source is eclipsed. The top panel in Fig. 1 shows the *RXTE*-ASM light curve in the 2–10 keV band, the middle panel shows the *Swift*-BAT light curve in the 15–50 keV band and the bottom panel displays the *Suzaku*-XIS light curve in the 0.2–12 keV band.

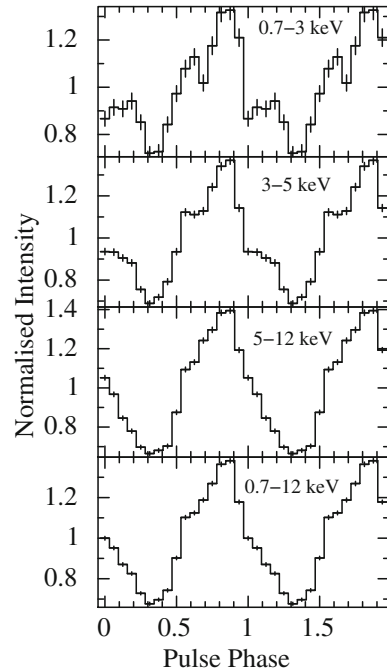


**Figure 3.** Energy-resolved pulse profiles of XTE J1855-026 in different energy bands folded with a pulse period of 360.01 s.

### 3. Timing analysis

For performing timing analysis for this dataset, we have applied barycentric corrections to the XIS cleaned event

<sup>1</sup><https://heasarc.gsfc.nasa.gov/docs/suzaku/analysis/abc/>

**Table 1.** Best-fitted time averaged spectral parameters of XTE J1855-026. Errors quoted here are for 90% confidence limits.

Parameter	Value
$N_{\text{H1}}$ ( $10^{22}$ atoms $\text{cm}^{-2}$ )	$5.90 \pm 0.05$
$N_{\text{H2}}$ ( $10^{22}$ atoms $\text{cm}^{-2}$ )	$16.82^{+0.82}_{-0.53}$
Cvfract	$0.63^{+0.007}_{-0.005}$
$P_{\text{index}}$	$1.12 \pm 0.01$
$P_{\text{norm}}^{\text{a}}$	$8.26 \pm 0.0004$
$kT_{\text{BB}}$ (keV)	$0.12^{+0.0009}_{-0.002}$
$kT_{\text{norm}}$	$1.82 \times 10^{-2} \pm 0.002$
$E_{\text{Fe}}$ (keV)	$6.42 \pm 0.005$
$\text{Fe}_{\text{norm}}^{\text{b}}$	$7.70 \pm 0.000006$
Iron line eq. width (eV)	$90 \pm 6$
Total flux (1.0–10.5 keV) <sup>c</sup>	5.28
Red- $\chi^2/\text{d.o.f}$	1.2/795

<sup>a</sup>  $\times 10^{-3}$  photons  $\text{cm}^{-2} \text{s}^{-1}$ ; <sup>b</sup>  $\times 10^{-5}$  photons  $\text{cm}^{-2} \text{s}^{-1}$ ; <sup>c</sup>  $\times 10^{-11}$  ergs  $\text{cm}^{-2} \text{s}^{-1}$ .

files using the ftool *aebarycen*. The light curves were then extracted with a time resolution of 8 s. The background subtracted light curves from all three XIS units were combined together for further analysis. The XIS light curve for this observation indicates that the count rate dropped by a large factor towards the end of the observation. We created background subtracted light curves and plotted with a bin size equal to the spin period of the pulsar  $\sim 360$  s in two different energy ranges, 0.3–5 keV and 5–12 keV, respectively as shown in Fig. 2 along with the hardness ratio. Light curves

show significant variations by a factor of up to 5 displaying increase in hardness ratios at certain intervals and towards the end of the observation.

We then searched for pulsations in the background subtracted light curves using the ftool *efsearch* by pulse folding and chi-square maximization technique. The pulse period was found to be 360.01 s. We then created energy resolved pulse profiles in four different energy ranges 0.7–3, 3–5, 5–12 and 0.7–12 keV respectively by folding the light curves with a period of 360.01 s and is shown in Fig. 3. The pulse profiles show little dependence with energy. The pulse profiles below 3 keV consist of an additional peak at phase 0.2 and a dip at phase 0.7 which gradually disappears above 5 keV and changed to a single peaked pulse profile similar to the averaged pulse profile 0.7–12 keV.

## 4. Spectral analysis

### 4.1 Time averaged spectral analysis

For analysing the energy spectrum of XTE J1855-026, after subtracting the background, spectrum from all the three XIS units were simultaneously fitted in the energy range 1.0–10.5 keV. Before fitting, each spectrum is grouped using ftool *grppha* in order to have a minimum of 20 counts per bin. The 2048 channel XIS spectra were further rebinned by a factor of 6 from 1 keV to 5 keV, by a factor of 2 from 5 to 7 keV and by a factor of 14 from 7 to 10.5 keV energy range. While

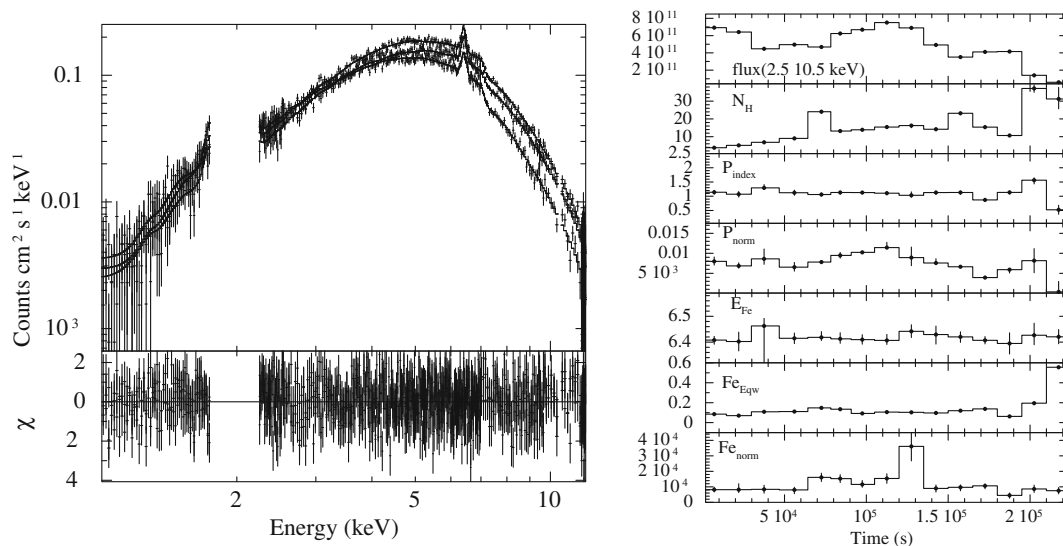


**Figure 4.** Left panel: The time-averaged energy spectrum of XTE J1855-026 with the best-fitted model components and the residuals obtained with the *Suzaku*-XIS detectors. Right panel: Variation in the spectral parameters with time is shown.

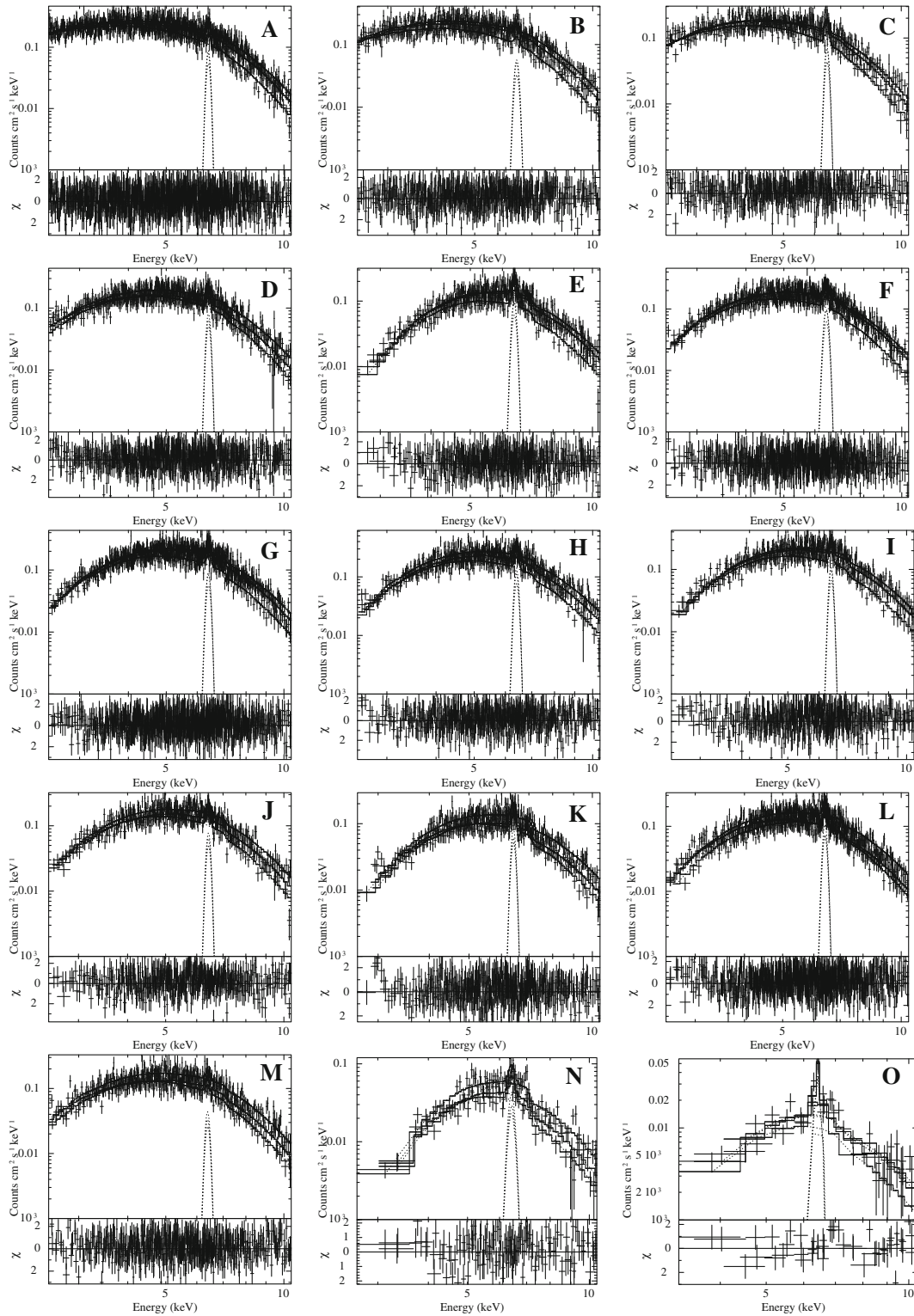


**Figure 5.** Time-resolved spectrum of XTE J1855-026 for different segments in the 2.5–10.5 keV energy range along with best-fitted spectral model and the residuals is shown.

fitting, all the spectral parameters other than the relative instrument normalization were tied together for all the three detectors. XIS spectra is known to have instrumental artifacts in the energy range 1.75–2.23 keV

and is ignored while fitting the spectrum. We first tried to fit the 1.0–10.5 keV energy spectrum with a model consisting of a simple absorbed power law model. This did not give a satisfactory fit with red- $\chi^2$  of 3.8.



Residuals at 6.4 keV indicate the presence of iron fluorescence line emission and a Gaussian function is included which gave a better fit. A low energy excess is obvious and a black body component was added (red- $\chi^2$  of 1.65). A partial covering absorption component is added which significantly improved the fit (red- $\chi^2$  of 1.22). We find that the energy spectrum of XTE J1855-026 in the energy range 1.0–10.5 keV was well fitted with a model consisting of partial covering power-law model, a black-body component for soft excess and a Gaussian function accounting for the iron fluorescence line emission and interstellar absorption. The best fitted spectral parameters of XTE J1855-026 are given in Table 1. The time averaged energy spectrum of XTE J1855-026 with the best-fitted model components and the residuals is shown in Fig. 4.

#### 4.2 Time-resolved spectral analysis

The hardness ratio plot shown in the bottom panel of Fig. 2 indicates significant absorption of soft X-rays at different times. To investigate the spectral variations in detail, we carried out time-resolved spectral analysis by dividing the entire Suzaku observation duration into 15 segments and created energy spectrum separately. Among these 15 segments, the last two segments N and O, are during the eclipse ingress. The duration of each segment is variable taking into account the variability of the hardness ratio carefully and are marked in Fig. 2. For fitting energy spectrum of each segment, we ignored the energy range below 2.5 keV due to limited statistics and hence the black body and partial covering component are not required. So the time-resolved spectrum for each segment is fitted with a simple absorbed power-law model and a gaussian function for iron fluorescence line emission. The variation of spectral parameters with time are shown in Fig. 4. We see that the column density and iron line equivalent width parameters vary significantly with time. An increase in hydrogen column density and iron line equivalent width is noticed with significant correlation with the variations observed in the hardness ratio plot. The variation in the hydrogen column density and iron equivalent width provide us with more insight into the distribution of the matter surrounding the system. The time-resolved energy spectrum of XTE J1855-026 for each segment with the best-fitted model components and resolution is shown in Fig. 5.

Figure 6 shows the variation in the shape of the continuum spectrum in three different segments B, E and N plotted together in a single panel showing the extremes

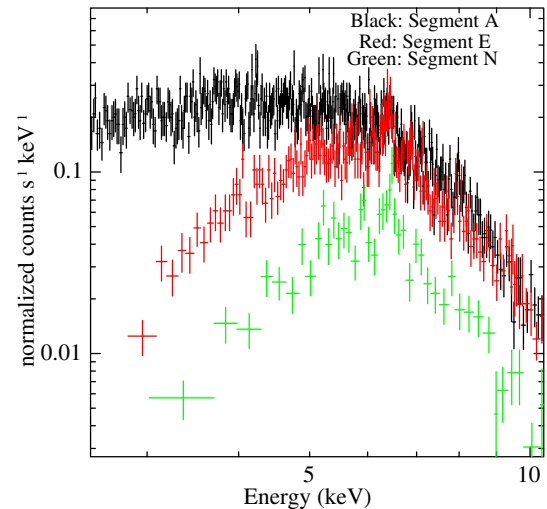


**Figure 6.** Variation in the shape of the continuum due to significant absorption of soft X-rays in three different segments obtained from the time resolved spectroscopic analysis.

of variation in the absorption of soft X-rays. The segments N and O are during eclipse ingress and show very low flux and very large equivalent width of iron line.

## 5. Discussion

In the previous sections, we have presented a detailed analysis performed on the *Suzaku*-XIS data of XTE J1855-026. The important results obtained give insight into the distribution of the surrounding matter. In stellar wind-driven accreting systems, the neutron star may be embedded in the material lost by the donor star and the inhomogeneities in the distribution of material in the form of clumps which will cause significant absorption of soft X-rays, especially when the system is in eclipse ingress or egress phase. The emitted X-ray radiation from the primary star can affect the structure and ionization of the stellar wind which in turn affect the velocity and density profile of outflows from the massive stars.

The important outcomes of the analysis are

- Even though the pulse profiles do not show significant energy dependence above 3 keV, at energies  $\leq 3$  keV, the pulse profile is characterized with an additional small peak along with the main peak. A little energy dependence and sharp features in the pulse profiles of XTE J1855-026 during flares using observations carried out with *RXTE*-PCA was reported by Corbet *et al.* (1999).

- The long-term orbital intensity profiles of XTE J1855-026 (Fig. 1) show significant energy dependence (Falanga *et al.* 2015). We noticed that the X-ray emission from the primary star got significantly reduced, even before the source went into eclipse. The very large  $N_{\text{H}}$  in the last two segments are probably due to the line-of-sight to the neutron star coming very close to the companion star surface where the stellar wind density is high. In segment E in which the X-ray intensity is low and  $N_{\text{H}}$  is high, as seen in Fig. 4, it is probably due to a clump in front of the neutron star. This indicates the presence of dense absorbing material in the near by surroundings and inhomogeneities in the stellar wind. Asymmetries in eclipse ingress and egress are reported in other supergiants like 4U 1700-37, Vela X-1, 4U 1538-52, OAO 1657-415 (Falanga *et al.* 2015 and references therein). The energy dependent light curves of the eclipse ingress/egress of the classical sgHMXBs reveal details of the OB stellar wind structure where it can be caused by accretion wakes.
- Classical sgHMXBs are known to show significant variations in the spectral parameters which indicates the presence of dense stellar wind surrounding the compact object. Flaring activity and short off-states have been observed in Vela X-1 which were interpreted as the effect of a strongly structured wind, characterizing the X-ray variability of Vela X-1 with a log-normal distribution, interpreted in the context of a clumpy stellar wind (Fürst *et al.* 2010). Few known sources with clumpy stellar wind are OAO 1657-415 (Pradhan *et al.* 2014), 4U 0114+65 (Pradhan *et al.* 2015), Cen X-3 (Naik *et al.* 2011), Vela X-1 (Fürst *et al.* 2010) and GX 301-2 (Islam & Paul 2014). Time-resolved spectral parameters of XTE J1855-026 showed significant variations with time, especially for the equivalent hydrogen column density ( $4\text{--}36 \times 10^{22}$  atoms  $\text{cm}^{-2}$ ) and iron line equivalent width (84–509 eV). In accretion powered pulsars, the Fe  $K\alpha$  line is produced by the reprocessing of the hard X-ray emission in the relatively low ionized and cool matter surrounding the pulsar. The increase in line equivalent width corresponds to the increase in the number of scattering on

passing through the dense matter. The presence of soft excess is detected in the phase averaged energy spectrum of XTE J1855-026. The soft excess is modelled with a black-body component which requires a temperature of 0.12 keV. Several other known sources which shows the presence of soft excess include SMC X-1, LMC X-4, RX J0059.2-7138 and X Per (Paul *et al.* 2002).

From this *Suzaku* observation, it is evident that the companion wind characteristics of XTE J1855-026 are similar to Vela X-1, OAO 1657-415, etc.

## Acknowledgements

This research has made use of data obtained from the *Suzaku* satellite, a collaborative mission between the space agencies of Japan (JAXA) and the USA (NASA).

## References

- Corbet R. H. D., Mukai K. 2002, *ApJ*, 577, 923  
 Corbet R. H. D., Marshall F. E., Peele A. G., Takeshima T. 1999, *ApJ*, 517, 956  
 Falanga M., Bozzo E., Lutornor A., Bonnet-Bidaud J. M., Fetisora Y., Puli J. 2015, *A&A*, 577, 130  
 Fürst F., Kreykenbohm I., Pottschmidt K., Wilms J., *et al.* 2010., *A&A*, 519, A37  
 Gonzalez-Galan A. 2015, [arXiv:1503.1087](https://arxiv.org/abs/1503.1087)  
 Islam N., Paul B. 2014, *MNRAS*, 441, 2539  
 Koyama K. *et al.* 2007, *PASJ*, 59, 23  
 Krimm H. A. *et al.* 2012, *ATel*, 3964, 1  
 Mitsuda K. *et al.* 2007, *PASJ*, 59, 1  
 Naik S., Paul B., Ali Z. 2011, *ApJ*, 737, 79  
 Negueruela I., Casares J., Verrecchia F., Blay P., Israel G. L., Covino S. 2008, *ATel*, 1876, 1  
 Paul B., Nagase F., Endo T., Dotani T., Yokogawa J., Nishiuuchi M. 2002, *ApJ*, 579, 411  
 Pradhan P., Maitra C., Paul B., Islam N., Paul B. C. 2014, *MNRAS*, 442, 2691  
 Pradhan P., Paul B., Paul B. C., Bozzo E., Belloni T. M. 2015, *MNRAS*, 454, 4467  
 Takahashi T. *et al.* 2007, *PASJ*, 59, 35  
 Watanabe K., Bozzo E., Mereghetti S., Gotz C. B. D. 2010, *ATel*, 2482, 1